HYDRATION AND PROPERTIES OF BLENDED CEMENT SYSTEMS INCORPORATING INDUSTRIAL WASTES

#MOHAMED HEIKAL*, **, H. EL-DIDAMONY***, M. A. MOUSTAFA***

*Chemistry Department, Faculty of Science, Benha University, Benha, Egypt
** Chemistry Department, Faculty of Science, Al-Imam Muhammad ibn Saud Islamic University, Riyadh, Saudi Arabia
***Chemistry Department, Faculty of Science, Zagazig University, Zagazig , Egypt

#E-mail: ayaheikal@hotmail.com

Submitted September 3, 2012; accepted June 16, 2013

Keywords: Blended cement, Ground clay bricks, Blast furnace slag, Silica fume, Ternary blended system

This paper aims to study the characteristics of ternary blended system, namely granulated blast-furnace slag (WCS), from iron steel company and Homra (GCB) from Misr Brick (Helwan, Egypt) and silica fume (SF) at 30 mass % pozzolanas and 70 mass % OPC. The required water of standard consistency and setting times were measured as well as physico-chemical and mechanical characteristics of the hardened cement pastes were investigated. Some selected cement pastes were tested by TGA, DTA and FT-IR techniques to investigate the variation of hydrated products of blended cements. The pozzolanic activity of SF is higher than GCB and WCS. The higher activity of SF is mainly due to its higher surface area than the other two pozzolanic materials. On the other side, GCB is more pozzolanic than WCS due to GCB containing crystalline silica quartz in addition to an amorphous phase. The silica quartz acts as nucleating agents which accelerate the rate of hydration in addition to its amorphous phase, which can react with liberating $Ca(OH)_2$ forming additional hydration products.

INTRODUCTION

The problem of producing pozzolanic, and filled-pozzolanic cements, has been of considerable scientific and technological interest because such additions increase the chemical resistance to aggressive attack, impermeability, lowering heat of hydration and thermal properties. The pozzolanic cements are increasing worldwide because they need less energy for production [1]. Cement containing fly ash, calcined clay, granulated blast-furnace slag, steel slag or silica fume are the key ingredients for high performance concrete.

Ground granulated blast-furnace slag (WCS) is an industrial by-product of the iron making process and is produced by water quenching molten blast furnace slag. For its use in pozzolanic cements, it must be ground with cement to improve its reactivity during cement hydration. Slag shows primarily cementitious behavior but may also show some pozzolanic character (reaction with lime) or has latent hydraulic properties. Replacement of clinker by slag not only offers energy savings and cost reduction compared to OPC, but also other advantages such as low heat of hydration, high sulphate, chloride and acid resistance, better workability, and good ultimate strength. Attempts have been made to overcome the problem of slow strength development in Portland slag cement through fine grinding and mechanical activation of the pozzolanic cement constituents [2, 3].

Homra (GCB) is a solid waste materials produced from the manufacture of clay bricks and shows slow rate as well as low heat of hydration. In Egypt about 5 - 10 % Homra is a waste product. The utilization of this industrial by-product is widely used; to reduce cost, energy and pollution. Homra constitutes mainly of silica quartz, aluminosilicate, anorthite, hematite and anhydrite [4-6]. Therefore, it acts as a good pozzolanic material and as a filler in filled pozzolanic cement [7]. It shows resistance to aggressive media such as sulphates and chlorides in Portland and sulphate resisting blended cements as well as fire resistance [8-10].

The hydration of cement paste, comparing with that of pure cement paste is effected when fly ash or silica fume is added. Fly ash increases the initial hydration of cement, but prolongs the dormant and acceleration periods. Silica fume also accelerates the initial hydration, but prolongs the dormant period at low water to binder ratio [11, 12]. However both fly ash and silica fume enhance the hydration of cement at later ages, the rate of hydration of the blended system is reduced with fly ash and silica fume contents [13]. Since the pozzolanic reactions of fly ash and silica fume occur later and slowly, the pozzolana plays only as inert filler in the early age [14].

Proton NMR spin-lattice relaxation ($T1$) was used as a prober for observing the hydration of fly ash and silica fume blended cement pastes during the early

age [15]. The hydration of blended cement pastes was retarded by the addition these pozzolanas. However, the hydration rate of the cement blends was promoted. Silica fume was prone to form agglomerations during dormant period, by which some of the water was enclosed. Thus, the water was slowly consumed and also the signals intensity decreased slowly. At stage 3, because the silica fume particles provided precipitation sites for CSH gel, the hydration of cement was promoted. The hydration process of fly ash and silica fume-blended cement pastes was studied. It was shown that both the fly ash and silica fume retarded the hydration and prolonged the dormant period. Due to the change between ettringite and monosulfate, the curves presented 'shoulders' from 7 h to 12 h during the acceleration period. It was indicated that the hydration of blended cement pastes was promoted by the addition of fly ash and silica fume.

The effect of active silica fume or rice husk ash on the mechanical and physico-chemical characteristics of cement pastes made of Portland blast-furnace slag cement (PSC) with cement kiln dust (CKD). Blends made of PSC and CKD, improved by SF or RHA [16]. The partial substitution of PSC by 10 % and 15 % of CKD increases the rate of hydration and a subsequent improves compressive strength of hardened PSC–CKD pastes. In addition, the replacement of PSC, in PSC–CKD blends, by 5 % active silica was accompanied by further improvement of the physico-mechanical characteristics of the hardened PSC–CKD pastes.

Nataraja and Nalanda [17] investigated a variety of slag, fly ash, and cement dust in the performance of industrial by-products in controlled low-strength materials. Blended cements prepared from fly ash, calcined clay, micro silica, granulated slag, etc., are the best cementitious materials. This class of cements improves long-term strength and durability [18]. Mechanisms of slag hydration in slag cements was discussed [19]. Slag grains develop membranes that control diffusion and densify the paste matrix that exhibits low permeability; $Ca(OH)_2$ is consumed by slag grains and Mg content forms hydrotalcite.

Blended cement mortars with fixed workability from blast furnace slag and silica fume, were tested for compressive strength and mercury intrusion. The results showed that with high portions of slag and silica fume, the mortars reached relatively satisfactory level of compressive strength and contributed to the significantly denser pore structure [20]. The binding system with cement-slag-silica fume is similar to that of only silica fume, because the effect of slag in blends is superimposed to the more expressive effect of silica fume. The presence of slag in ternary blends that increases the water demand due to the silica fume fineness appears not to be so expressed as in cement-silica fume mortars and hence, the drop in compressive strength due to the increased w/b ratio is significantly lower.

The goal of the present investigation aims to use condensed silica fume (SF), granulated blast furnace slag (WCS) and Homra (GCB) by-products such as for the preparation of blended cements. The hydration characteristics of these blended cements were also studied up to 3 months. They help to reduce the cost and conserve energy sources, and the environment.

EXPERIMENTAL

The materials used in this investigation were ground granulated blast furnace slag (WCS), which provided from iron steel company, Helwan, Homra (GCB) from Misr Brick, Helwan, silica fume (SF) from Ferrosilicon Alloys Company, (Edfo, Aswan, Egypt) and ordinary Portland cement (OPC) from Suez cement Company; Egypt. The chemical oxide compositions of each starting materials are given in Table 1. The surface area of each material was determined using Blaine apparatus which is shown in Table 1. The mix compositions of the investigated pastes are given in Table 2.

Table 2. Mix composition of the investigated specimens, mass %.

Mix No.	OPC	GCB	WCS	SF
OPC	100	–	–	–
H1	70	–	–	30
H2	70	10	–	20
H3	70	20	–	10
H4	70	30	–	–
F0	70		30	–
F1	70		20	10
F2	70		10	20
S1	70	10	20	–
S2	70	10	10	10

Table 1. Chemical composition of starting materials, mass %.

	SiO_2	Al_2O_3	Fe_2O_3	CaO	MgO	MnO	TiO_2	Na_2O	K_2O	BaO	SO_3	S^{2-}	L.O.I	Surface area ($m^2\ kg^{-1}$)
WCS	37.48	12.86	0.40	36.70	2.45	6.24	0.72	1.84	0.71	5.31	0.01	0.75	--	350
OPC	21.51	5.07	4.39	65.21	2.00	0.15		0.23	0.29		0.25		0.40	310
SF	96.10	0.52	0.70	0.21	0.48	--	--	0.31	0.49	--	0.10	--	1.14	2500
GCB	74.80	14.03	5.04	1.25	1.30	--	--	--	--	--	0.80	--	--	300

The dry constituents were mechanically mixed for one hour in a porcelain ball mill using three balls to attain complete homogeneity, and kept in airtight containers. The mixing of the cement paste was carried out with the required water of standard consistency. The blended cement was placed on a smooth non-absorbent surface and a crater was formed in the center. The required amount of water was poured into the crater by the aid of a trowel. The dry cement around the outside of the crater was slightly troweled over the remaining mixture to absorb the water for about one minute. The mixing operation was then completed by continuous vigorous mixing for about three minutes by means of gauging trowel. At the end of mixing, the paste was directly poured in 2 cm cubic moulds pressed and smoothened with the aid of the trowel. The cubes were cured in humidity chamber for 24 hours then demoulded and continuously cured under water until the time of investigation.

The water of consistency, initial and final setting time of cement pastes were determined using a vicat apparatus [21]. The hydration of cement pastes was stopped using microwave oven. The cement pastes were placed in suitable container (glass dish). The apparatus used was microwave oven (EM-S3555, Sanyo, China, living technology). The glass dish containing the cement specimen placed in a microwaves oven for 10 minutes to remove the free water. The kinetic of hydration was followed by the determination of combined water contents from the ignition loss of dried sample. The hydration products were followed using DTA, TGA and FT-IR spectroscopy. The total porosity, bulk density and compressive strength of cement pastes were also measured.

The bulk density was carried out before the pastes subjected to compressive strength determination. Bulk density was determined through weighing the hardened pastes (suspended in water) and in air (saturated surface dry). Each measurement was conducted on at least three similar cubes of the same age [22]. The total porosity (ε) was determined from the evaporable (We), total water (W_t) contents and bulk density (dp) of the hardened cement specimen using the following equation [22]:

$$\varepsilon = \left(\frac{0.99\ We \times dp}{(1 + Wt)} \times 100 \right)$$

A set of three cubes was used for the determination of compressive strength of cement paste (ASTM Designation: C-150, 2007). The compressive strength measurements were done on a compressive strength machine of SEIDNER, Riedinger, Germany, with maximum capacity of 600 KN force.

The free lime content of cement paste can be thermally determined. 0.5 g of the hardened cement was placed in a porcelain crucible and introduced into a cold muffle furnace. The temperature was increased up to 390 then to 550°C at heating rate of 3°C/min. The loss of weight occurred between 390 - 550°C with soaking time of 15 min is equal to the weight of water of calcium hydroxide. Therefore, the free lime can be calculated.

The combined water content is considered as the percent of ignition loss of the dried samples (on the ignited weight basis). Approximately 2 g of the predried sample were gradually ignited up to 1000°C for 1 hour soaking time. The results of combined water were corrected form the water of free lime present in each sample [22].

The samples were prepared using alkali halide pressed disk technique as it gives a further reduction in scattering [23]. 2 mg of the sample was ground with 198 mg of potassium bromide in an agate mortar to produce a homogeneous mixture. The mixture pressed under vacuum to give a transparent disc of 1cm in diameter. The infrared spectral analysis was recorded from KBr-discs using Genesis -IR spectrometer in the range 400 - 4000 cm^{-1}.

RESULTS AND DISCUSSION

Ground clay bricks and silica fume blended cement

Water of consistency and setting times

The water of consistency of neat OPC was 27 %. Replacement OPC by 30 % GCB (H4), the water of consistency increases to 28.7 %. The required water of standard consistency increases with SF content, due to the high surface area of SF (2000 - 2500 m^2/kg) in comparison with GCB (350 m^2/kg). The water of consistency, initial and final setting times are graphically plotted as a function of silica fume replacement instead of GCB in Figure 1. As the SF content increases, the water of consistency increases.

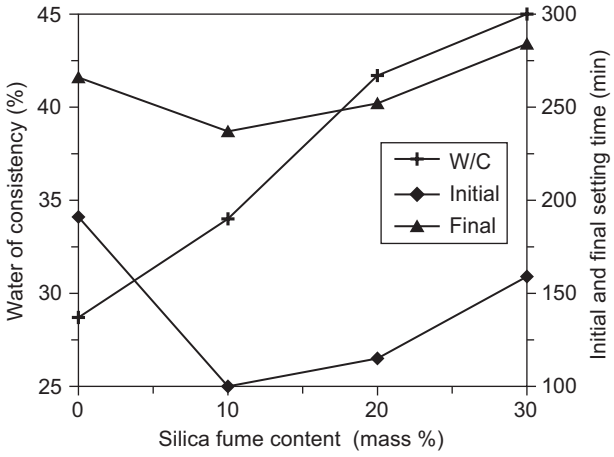

Figure 1. Water of consistency, initial and final setting time of blended cement pastes as a function of silica fume instead of GCB.

Replacement of 10 mass % GCB with SF accelerates the hydration of cement paste, due to the activity of SF in comparison with GCB. Therefore the initial setting is

shortened. The increase of SF on the expanse of GCB the initial and final setting time is elongated due to the increase of water of consistency, i.e. the mixing water increases the total porosity and initial setting time is elongated. The final setting time is nearly parallel the initial setting time.

The water of consistency increases due to high surface area of SF, which needs more water to produce standard consistency [24]. The initial and final setting times of blended cement pastes are graphically represented in Figure 1. As SF content increases the initial setting time diminishes, where the final setting elongates. The decrease in initial setting time is due to the nucleating agent of SF to activate the OPC cement phases [25-27]. As the SF increases the initial setting time increases up to 30 mass % due to the increase of mixing water. The final setting time is slightly elongated, due to high mixing water.

Chemically combined water contents

Chemically combined water contents of GCB and SF blended cement pastes cured up to 90 days are graphically plotted in Figure 2. The chemically combined water contents increase with curing time. It is clear that, the chemically combined water content of blended cement pastes with 30 % mass GCB show lower values than neat OPC pastes. This is due to that the C–S–H formed from the pozzolanic reaction of SF with CH, has lower water content than that formed from the OPC. As SF content increases the chemically combined water content increases due to the higher pozzolanic activity of SF in comparison with GCB. SF reacts quickly with CH forming additional C–S–H, where the rate of reaction of GCB is somewhat slow especially at early ages or may be due to formation a coating film on the grains of GCB. Zhang and Gjorv [28] investigated the effect of SF on the hydration of cement in low-porosity cement pastes. For cement pastes of low water/cement (w/c) ratio (≤ 0.4), only a moderate increase of combined water content during a period of ≤ 550 days was observed. In the presence of SF combined water decreases from 90 - 550 days. This is assumed to be due to a release of water during polymerization of the silicates [29, 30]. The pozzolanic reaction starts even before one day and continues to ≤ 550 days. The reaction kinetics are much effected by w/c ratio. For decreasing w/c ration from 0.4 to 0.2, $Ca(OH)_2$ contents of ~ 16.12, and 8 % were observed respectively. At 16 % replacement, $Ca(OH)_2$ was completely consumed regardless of the w/c ratio.

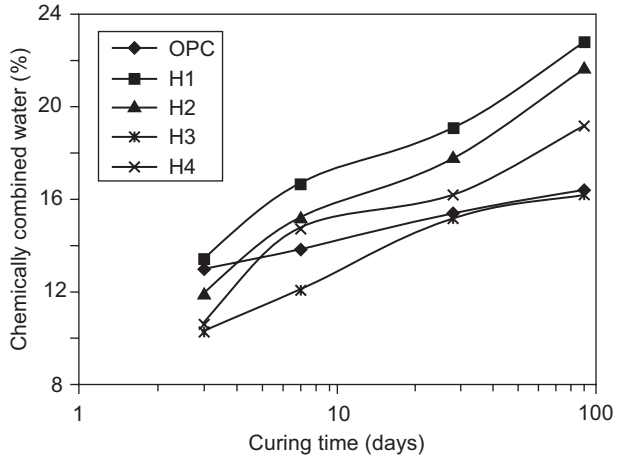

Figure 2. Chemically combined water contents of OPC and blended cement as a function of SF replacement instead of GCB up to 90 days.

DTA and TGA

Figure 3 shows the thermograms of OPC and blended cement pastes H_2, H_3 and H_4 cured up to 90 days. The thermograms have five endotherms and one exothermic peak. The first three endotherms at 80, 110 and 140°C are attributed to the dehydrated of moisture interlayer of calcium silicate (C–S–H), calcium aluminate (C–A–H) and calcium sulphoaluminate hydrates. As the SF content increases the area under these peaks increases up to 20 % SF. The peak located at 490°C is due to the dehydroxlation of $Ca(OH)_2$. As the SF content increases the peak area decreases, due to the increase in pozzolanic activity of silica fume to react with residual lime to produce additional calcium silicate hydrates. The endothermic peak located at 763°C is due to the decomposition of $CaCO_3$. The exothermic peak ocurred at 944°C is mainly characteristic of calcium silicate which is developed during the crystallization of mono-

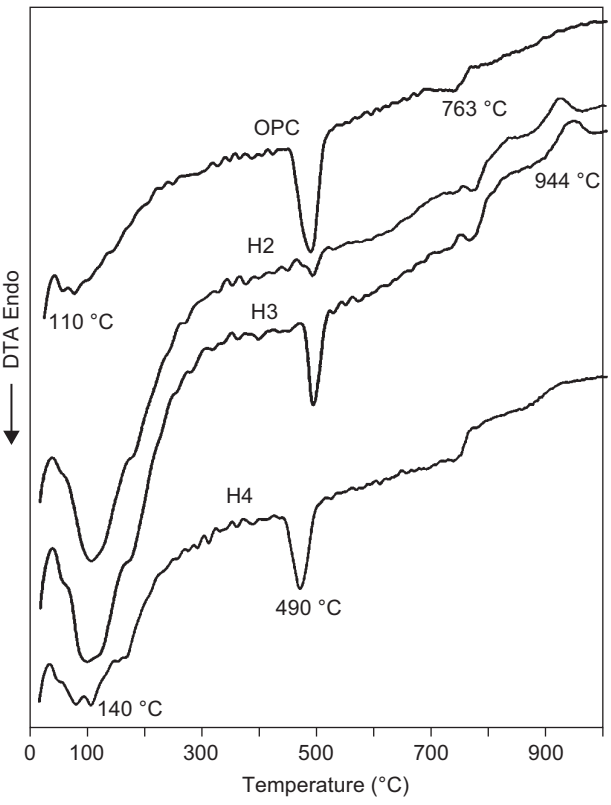

Figure 3. DTA thermograms of OPC and blended cement pastes cured at 90 days.

calcium silicate (Wallostonite) [31]. As the silica fume content increases (mix H2 and H3) more crystallization of the monocalcium silicate ($CaO{\cdot}SiO_2$) represented at 944°C. The peak area of the hydrated phases decreases with SF content. Also, OPC pastes show the higher value of portlandite as shown from the peak area at 490°C. It is clear that SF is more hydraulic than GCB as shown from the low thermal peaks of the hydration products.

Figure 4 shows the weight loss of hydrated phases from TGA thermograms of OPC and blended cement pastes containing 10, 20, and 30 SF cured for 90 days. The thermograms show three temperature ranges up to 390°C due to the decomposition of C–S–H, CAH and hydrogarnet phase. The peak located at 400 - 520°C is due to the decomposition of CH, the last endothermic peak at 650 - 800°C due to the decomposition of $CaCO_3$. The peak located up to 390°C increases the decomposition of the hydration products with SF up to 10 - 20 mass %, then the amount of C–S–H increases due to the pozzolanic

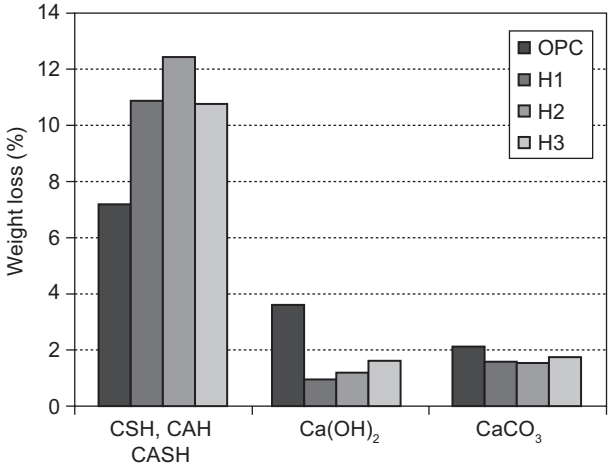

Figure 4. Weight loss of hydrated phases from TGA thermograms of OPC and blended cement pastes with 10, 20 and 30 SF instead of GCB up to 90 days.

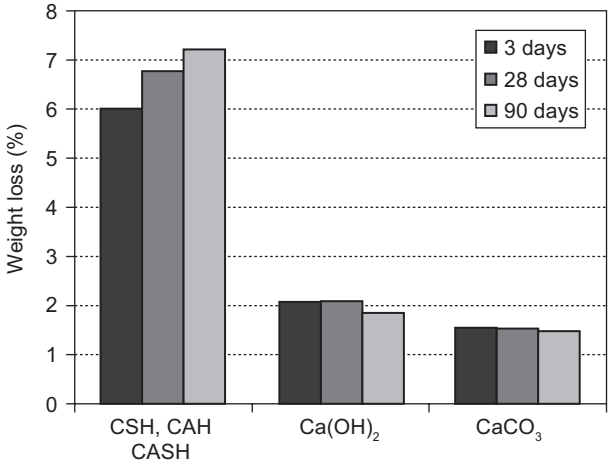

Figure 5. Weight loss of the decomposition of 30 % SF cement from TGA thermograms of cured at 90 days.

activity of SF. On the other hand it was shown that 30 mass % SF show lower values than 10 and 20 mass % in presence of GCB. This is also due to the low water content of C–S–H from the pozzolanic reaction of SF with CH. OPC pastes have higher values than blended cement pastes, due to pozzolanic reaction of SF and GCB which consumed CH in the pozzolanic reaction, hence the residual lime decreases. The loss on weight at 600 - 800°C decreases, i.e. the OPC pastes is more carbonated due to the increase the amount of portlandite in comparison to blended cement pastes or the decrease of OPC content. Also, it was found that as the SF content increases the weight loss of portlandite and $CaCO_3$ decreases up to 30 mass % SF.

Figure 5 shows the weigh loss of hydrated phases from TGA thermograms of cement pastes containing 30 mass % SF. As the curing time increases, the weight loss from the decomposition of C–S–H and CAH as well as CASH increases. The weight loss from the decomposition of $Ca(OH)_2$ and $CaCO_3$ decreases with curing time, due to the pozzolanic reaction of SF with liberated $Ca(OH)_2$ to produce additional C–S–H which precipitated within the pore system to increase the compressive strength. Also, as the portlandite decreases the $CaCO_3$ also decreases.

FT-IR spectra of hydrated cement pastes

Figure 6 shows FT-IR spectra of hydrated cement pastes containing 0, 10, 20, 30 mass % SF cured up to 90 days. FT-IR spectroscopy is one of the most powerful techniques normally used for molecular characterization. In particular, the FT-IR results are used to resolve the hydroxyl bands and to monitor the dynamic changes in the water region during the hydration reaction [32]. There are three bands in the region 3800 - 3100 cm^{-1}, $Ca(OH)_2$ gives a peak at 3644 cm^{-1}, ettringite has one band at 3420 cm^{-1} and a weak band at 3600 cm^{-1}, and 3600 cm^{-1}, and monosulphate has one at 3100, 3500 (broad) 3540 and 3675 cm^{-1}. The broad band centered at 3494 cm^{-1} is due to symmetric and asymmetric ($v_1 + v_2$) stretching vibration of O–H water. The water stretching region (≈ 3490 - 3440 cm^{-1}) becomes broader with curing time; this is due to the molecular water. The bending vibration of water can be seen at 1642 cm^{-1}.

The carbonate bands located at 1428 cm^{-1} arise from the atmosphereic CO_2 with the residual $Ca(OH)_2$ [33] and v_2 due to CO_3^{2-} (878 cm^{-1} and v_3 CO_3^{2-} 712 cm^{-1}). The small peak located at 1120 - 1180 cm^{-1} is due to v_3-SO_4^{2-}, supported the presence of ettringite and monosulphate hydrate. The ettringite phase is the major hydration products at the early ages.The broad bonds at 3494 cm^{-1} related to the symmetrical stretching frequencies v_2-H_2O. This band for H_2O increases with curing time up to 90 days due to the large incorporation of H_2O molecules in the formation of hydration products, such as C–S–H, CAH and CASH at 972 cm^{-1} and 876 cm^{-1}. This peak is

due to S–O–Al–O–.

From Figure 6 it has been found that as the SF content increases the band due to $Ca(OH)_2$ (3644 cm^{-1}), and the bands at 1428 and 876 cm^{-1} due to the decrease of CO_3^{2-} diminish for H_2 and H_1 (20 and 30 % SF). On the other hand, the broad band at 3494 cm^{-1} increases the peak due to S–O–, Al–O (972 cm^{-1}) becomes broader with the silica fume content, due to the formation of more CSH and CAH as well as CASH.

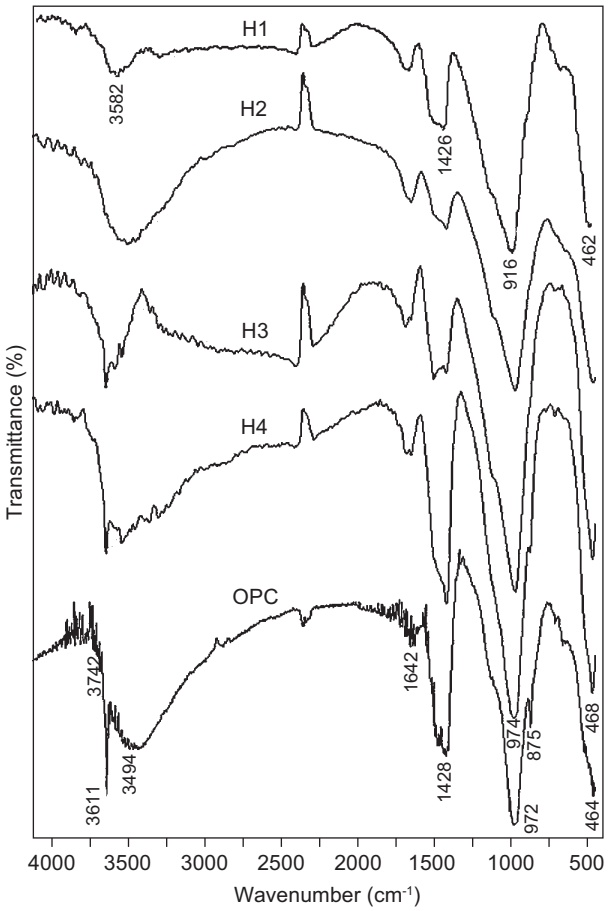

Figure 6. FT-IR spectroscopy of 0, 10, 20, 30 mass % SF-blended cement pastes up to 90 days.

Bulk density

The bulk densities of hardened cement pastes cured up to 90 days are given in Figure 7. As the SF content increases the bulk density decreases, due to the increase of the mixing water [27], accordingly the total porosity increases and then the bulk density decreases. Generally, the bulk density of any pozzolanic cement pastes is lower than that of OPC pastes. This is due the decrease of bulk density of pozzolanic cement in relation to OPC as well as the decrease of bulk density of C–S–H formed during the pozzolanic reaction in comparison with that of OPC [1]. As the hydration progresses, the hydration products fill a part of the pore volume, then the bulk density increases and total porosity decreases. It is clear that the bulk density of hardened cement pastes increases with curing ages. As the amount of SF increases the bulk density decreases due to the increase of water of consistency, which increases with SF. The initial water/cement ratio plays an important role in the values of bulk density.

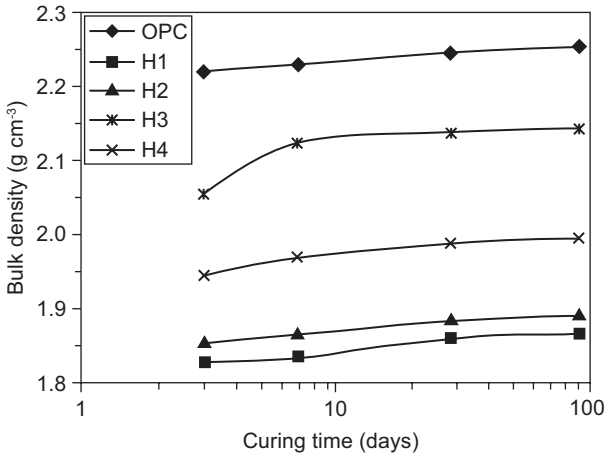

Figure 7. Bulk density of hardened GCB-SF cement pastes cured up to 90 days.

Total porosity

The total porosity of cement pastes are graphically plotted as a function of curing time in Figure 8. The total porosity of hardened cement pastes decreases with curing time. As the hydration precedes more hydration products are formed, which fill up some open pores, therefore the total porosity decreases.

At early age (3 - 7 days) pastes with 30 mass % GCB have higher total porosity than OPC pastes. But, at 28 - 90 days the total porosity is lower than that of OPC pastes. This is due to somewhat pozzolanic activity of GCB to produce additional C–S–H and CAH as well as CASH hydration products, which precipitated in some pores

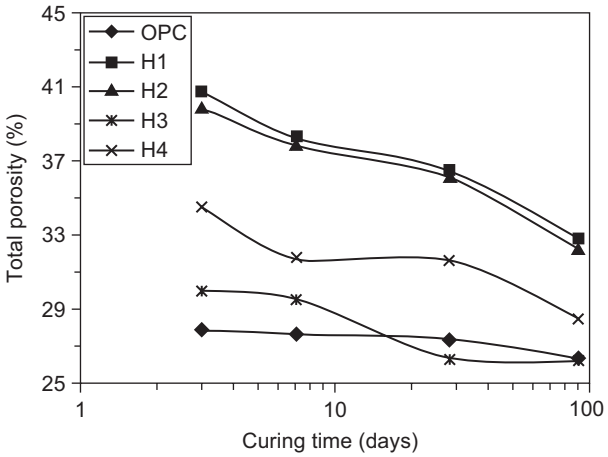

Figure 8. Total porosity of OPC and GCB-SF cement pastes up to 90 days.

to reduce the total porosity. Replacement of GCB by 10, 20 - 30 mass % SF, the total porosity increases respectively, due to the increase of the water of consistency. The data of total porosity and bulk density are in a good agreement.

Compressive strength

The compressive strength of OPC and blended cement pastes containing different ratios of SF and GCB (Homra) are graphically represented in Figure 9. The results indicate that the compressive strength increases with curing time for all cement pastes due to increase the amount of hydration products especially C–S–H, which is the source of compressive strength. The compressive strength decreases with SF content. The initial mixing water or the water of consistency increases with the SF content, therefore the evaporable water as well as the total porosity increase and the compressive strength decreases. The hydration products have a higher specific volume than unhydrated cements. Therefore, the hydrated products fill up some of the pores that lead to decrease the total porosity of pastes. In SF-blended cement pastes the chemically combined water increases with SF content and the total porosity decreases, these two factors work together to increase the compressive strength.

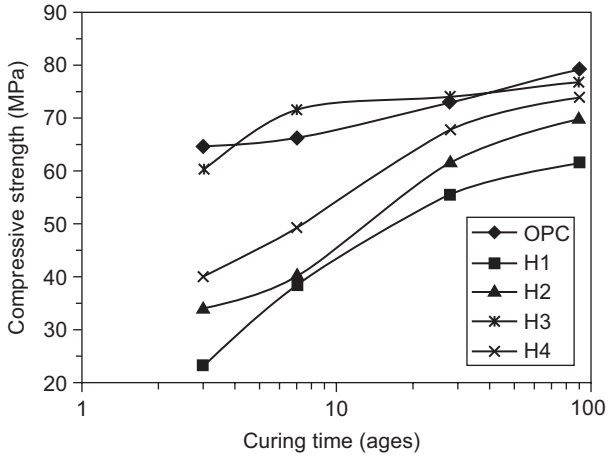

Figure 9. Compressive strength of OPC and blended cement pastes as a function of curing time up to 90 days of cement pastes.

Blended cements containing WCS and SF

Water of consistency and setting time

The water of consistency and setting times of cement pastes are graphically represented as a function of SF content in Figure 10. The water of consistency increases with SF content due to its high surface area which needs higher amounts of mixing water. The initial setting time was shorten by substitution of 10 mass % WCS by SF. Silica fume has higher pozzolanic activity than WCS, which reacts with residual $Ca(OH)_2$ to form more hydration products as a result of pozzolanic reaction. The replacement of 10 % WCS with SF tends to accelerate the initial setting time due to its nucleating effect [5, 25, 26]. Increase the amount of SF to 20 - 30 mass %, the initial setting time elongated. This is due to the higher amount of mixing water which delays the setting of cement paste. The final setting time is elongated with the silica fume content.

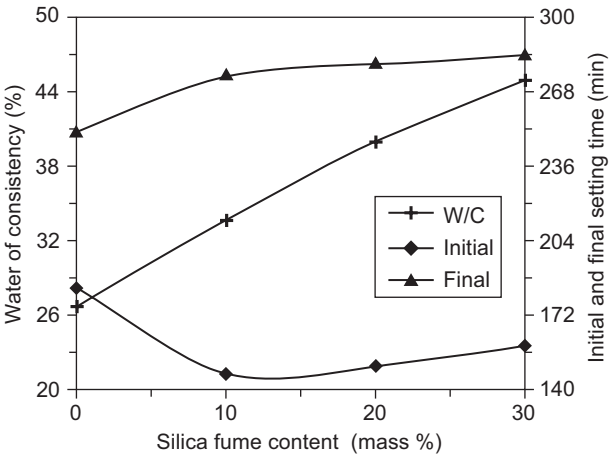

Figure 10. Water of consistency, initial and final setting times as a function of silica fume content.

Chemically combined water content

The chemically combined water contents of cement pastes are graphically plotted as a function of curing time as well as SF content in Figure 11. The chemically combined water content increases with curing time for all cement pastes. Replacement of WCS by SF the chemically combined water enhances due to the high surface area of SF and formation of C–S–H by the pozzolanic reaction with liberated lime. This leads to form more hydration products than those free from

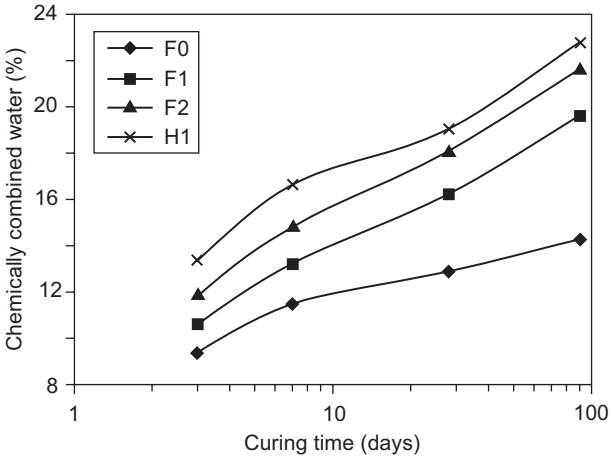

Figure 11. Chemically combined water contents of cement pastes containing WCS and SF.

SF. Silica fume reacts quickly with liberated $Ca(OH)_2$ to form the additional amounts of C–S–H, whereas the rate of hydration of WCS is slower. This is due to the formation of acidic surface films on the grains WCS. The rate of hydration is very slow, but it increases in alkaline media. As the hydration time increases the $Ca(OH)_2$ removes this film and the hydration proceeds, then the combined water increases [9].

DTA and TGA

Figure 12 shows the DTA thermograms of OPC and blended cement pastes containing F0 (30 mass % WCS) and F1 (20 mass % WCS + 10 mass % SF) cured up to 90 days. The endothermic peak below 200ºC is due to the decomposition of interlayer of calcium silicate, aluminate and aluminosilicate hydrates. The peak located at 486°C is due to the dehydroxylation of $Ca(OH)_2$, whereas the two peaks presented at 734 and 800°C are attributed to the decomposition of different forms of $CaCO_3$. In the presence of SF in mix F1, the peak area below 200°C, increases, where, the peak area at 480°C decreases, due to the reaction of SF with residual lime to form additional calcium silicate hydrate which is decomposed within peak below 200°C.

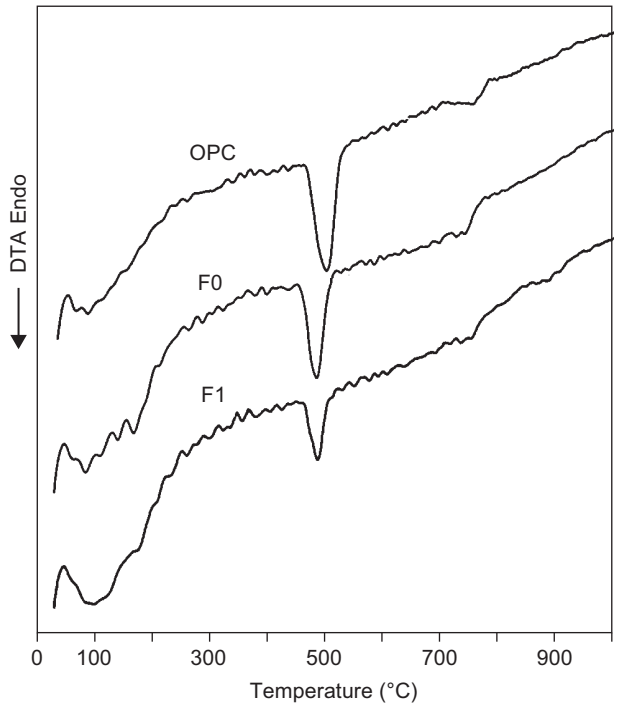

Figure 12. DTA thermograms of OPC and blended cement pastes containing F0 and F1 cured up to 90 days.

The weight loss of hydrated of cement pastes cured up to 90 days are given in Figure 13. The first step is due to the composition of calcium silicate, aluminate, sulphoaluminate and calcium aluminosilicate hydrates up to 390°C. It was shown that sample F0 (30 mass % WCS) gives weight loss 9.48 %, which is more than OPC paste which has 7.209 %, i.e. the blended pastes containing 30 % slag contains more calcium silicate, aluminate and aluminosilicate hydrates than OPC pastes. The weight loss of specimens containing F1 (20 mass % WCS + 10 mass % SF) and F2 (10 mass % WCS + 20 mass % SF) are higher than the other blended cement pastes. The weight losses corresponding to $Ca(OH)_2$ and $CaCO_3$ show that the specimens containing SF have lower values. This due to the consumption of $Ca(OH)_2$ in the formation of additional calcium silicate hydrates during the pozzolanic reaction. More consumption of $Ca(OH)_2$ is also converted during carbonation with atmospheric CO_2 to form $CaCO_3$.

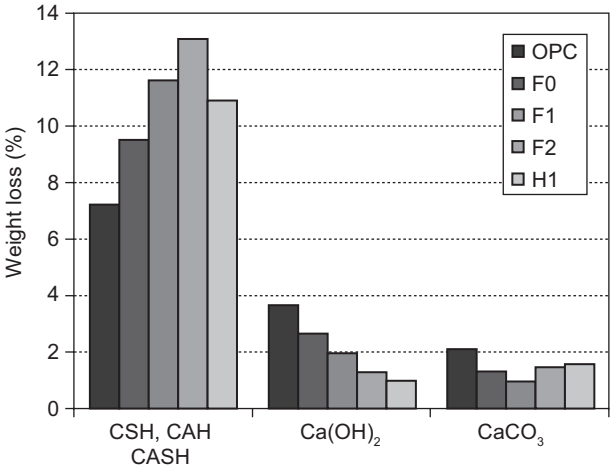

Figure 13. TGA thermograms of OPC and F0, F1, F2 and H1 cement pastes up to 90 days.

FT-IR spectra of hydrated cement pastes

Figure 14 shows the FT-IR spectroscopy of OPC and F0, F1 and H1 (30 mass % SF) cement pastes cured up to 90 days. The spectra are shown in three regions; the water, sulphate and silicate as well as aluminate regions. The broad bands centered at 3494 cm^{-1} are due to stretching vibration of O–H water molecule. The bending vibration of water molecule located at 1642 cm^{-1}. The band at 972 cm^{-1} as v_3 SiO_4 is due to the main hydration products of C–S–H, and CH from v O–H absorption band at 3644 cm^{-1}. The absorption band at 1428 cm^{-1} is due to the presence v_3 CO_3^{2-} as well as (v_2) 876 cm^{-1} and 712 cm^{-1} (v_5) that formed from the carbonation of $Ca(OH)_2$.

As the SF content increases the band located at 3494 and 1642 cm^{-1} was boarded. Also, the band at 3644 cm^{-1} diminished due to the decrease of the amount of $Ca(OH)_2$, as well as the band due to the carbonation (1428 and 876 cm^{-1}). This is due to the pozzolanic reaction of silica fume. On the other hand the band due to CSH increases with SF content and shifts to lower frequencies as indicated on the dissolve of the Si and Al to form CSH at 972 cm^{-1}.

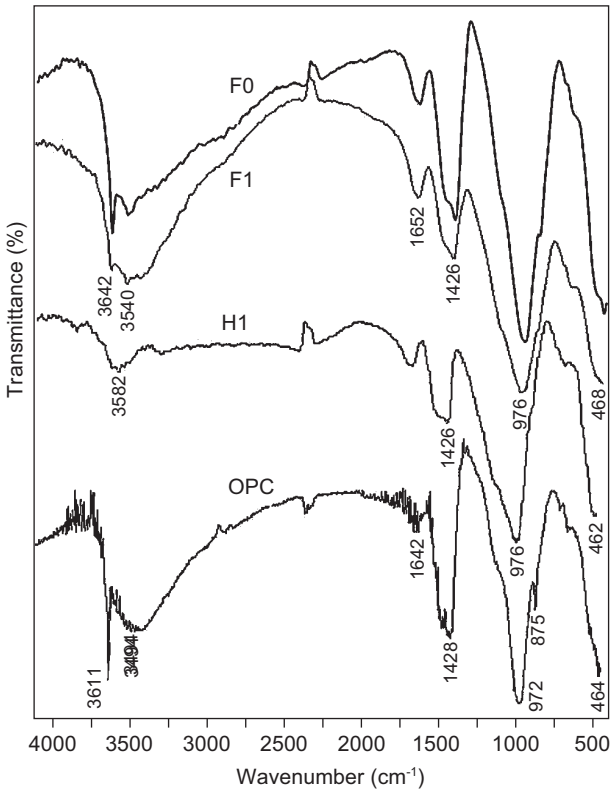

Figure 14. FT-IR spectroscopy of OPC and cement pastes containing F0, F1 and H2 cured for 90 days.

Bulk density

The bulk density of hardened cement pastes are shown in Figure 15. The bulk density of the cement pastes increases with curing time. The increase of SF content, the bulk density decreases, which is directly connected with the initial water of consistency that plays an important role to increase the total porosity and decrease the bulk density.

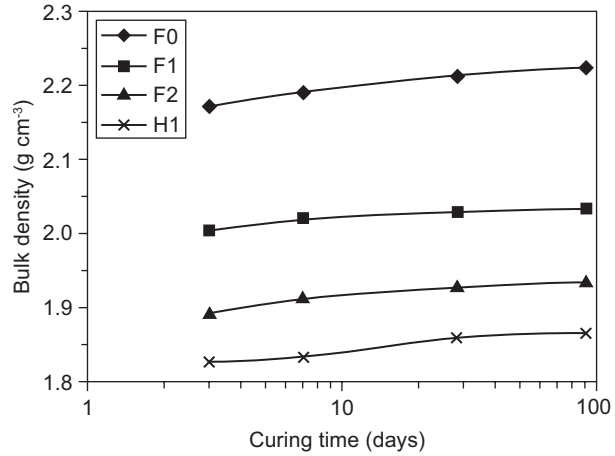

Figure 15. Bulk density of cement pastes containing SF instead of WCS up to 90 days.

Total porosity

The total porosity of hardened blended cement pastes are graphically plotted in Figure 16. The total porosity of cement pastes decreases with curing time. This is due to that the hydration products fill up some of the available pore volume. Replacement of SF content instead of WCS increases the water of consistency, therefore increases the total porosity.

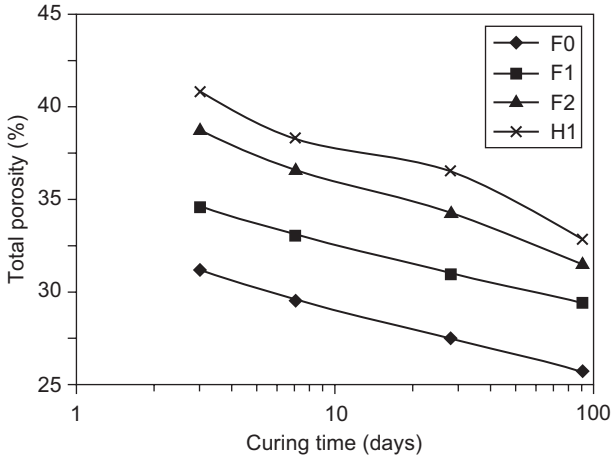

Figure 16. Total porosity of cement containing SF instead of WCS up to 90 days.

Compressive strength

Compressive strength values of hardened cement pastes cured up to 90 days are graphically represented in Figure 17. The substitution of WCS by SF in cement pastes containing 30 mass % WCS, the compressive strength decreases. The compressive strength increases with curing time for all hardened cement pastes. Also, as the SF content increases, the compressive strength decreases due to the high water of consistency. Total porosity increase and related bulk density decrease represent main factors responsible for compressive strength reduction.

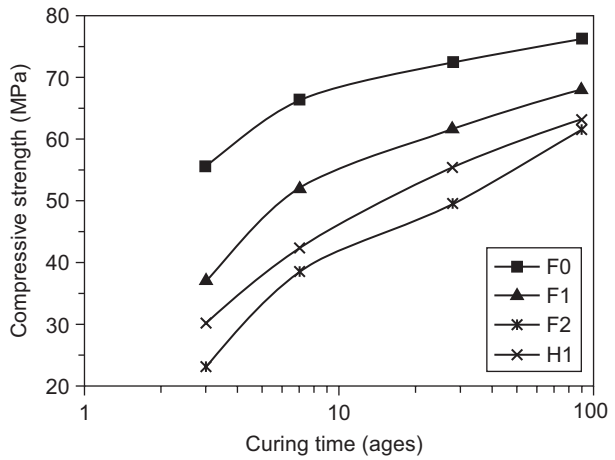

Figure 17. Compressive strength of hardened cement pastes containing SF instead of WCS cured up to 90 days.

Substitution of WCS with GCB and SF in blended cement

Water of consistency and setting times

Water of consistency, initial and final setting time of WCS with GCB and SF blended cement pastes are graphically represented in Figure 18. Water of consistency increases with the GCB and SF, due to the surface area of SF. S2 has the higher amount of water of consistency due to the replacement of 20 % WCS with 10 % GCB and 10 % SF. Both GCB and SF have the higher pozzolanity than WCS as shown previously in the first and second systems. The initial and final setting times elongate due to replacement of WCS by 10 mass % GCB (S_1). The initial setting time was elongated from 251 min to 312 min., whereas the final setting elongated from 184 min to 230 min. On the other hand, the initial and final setting times of S2 (10 % WCS + 10 % GCB + 10 % SF) were shortened. This is due to the presence of 10% SF, which acts as nucleating site, reacting with $Ca(OH)_2$ to produce more calcium silicate hydrates as well as accelerates the pozzolanic reaction, hence the initial and final setting of mix S2 are shortened (initial 162 min and final 257 min).

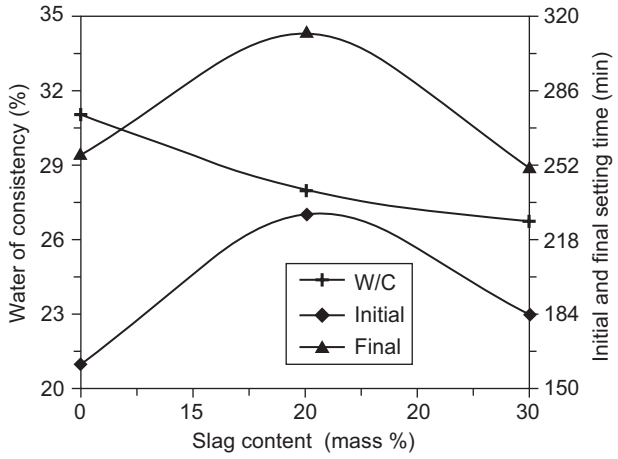

Figure 18. Water of consistency, initial and final setting times of WCS–GCB–SF cement pastes.

Chemically combined water contents

Chemically combined water contents are graphically represented in Figure 19. The chemically combined water contents increase with curing time for all cement pastes due to the progress of hydration. The combined water contents of blended cement pastes are higher than those of F0. This is due to the reactivity of SF and GCB comparison with WCS. Replacement of 10 mass % of WCS by 10 mass % GCB (S1), the chemically combined water contents were increased from 3 days up to 90 days. This is due to that GCB has higher hydraulic properties than the slag. Replacement 10 mass % WCS by 10 mass % SF, the mix S2 (10 mass % WCS + 10 mass % GCB + 10 mass % SF), the combined water content increases at early and later ages. The presence of SF enhances the hydraulic properties of mix S2 to form more additional CSH. SF reacts at early ages (3 days) with liberated $Ca(OH)_2$ to form more CSH, where as the hydration reaction of slag cement is somewhat delayed due to the formation of acidic surface films on the grains of WCS as small amounts of $Ca(OH)_2$ reacted, the hydration products such as CSH, CAH as well as CASH [9]. This elongates the reaction of WCS and CH.

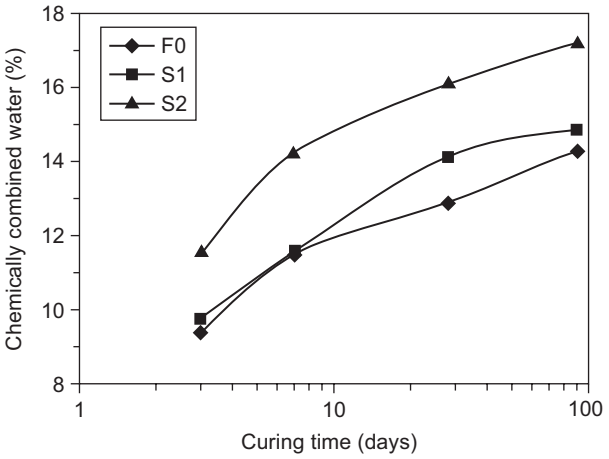

Figure 19. Chemically combined water contents of WCS–GCB–SF cement pastes up to 90 days.

FT-IR spectra of hydrated cement pastes

Figure 20 shows FT-IR spectra of hydrated cement pastes containing 70 % OPC + 10 % WCS + 10 % GCB + 10 % SF (S2) as a function of curing time. It is clear that the intensity of the band at 3649 cm^{-1} related to

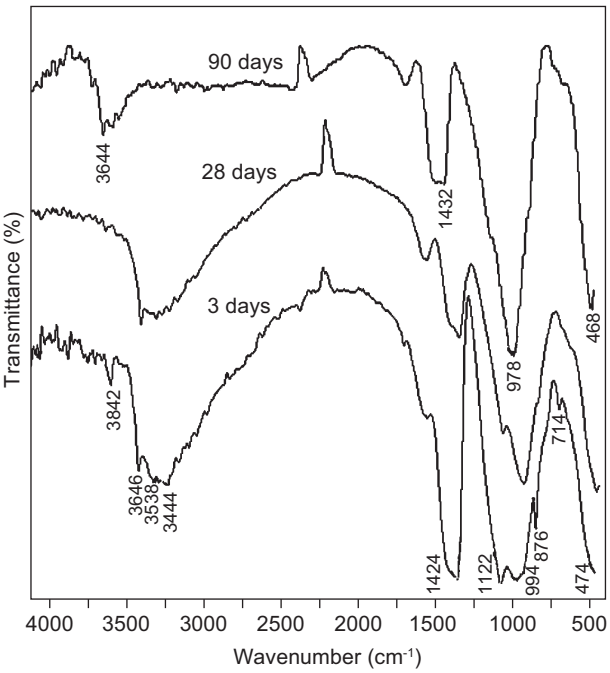

Figure 20. FT-IR spectroscopy of S2 pastes cured at 3, 28 and 90 days.

OH decreases with curing time up to 90 days. This is due to that the lime liberated from OPC cement phases reacts with active silica and alumina to from hydration products. The broad band near 3000 - 3538 cm^{-1} due to stretching band $v_1 + v_2$ of H_2O increases with curing time as a progress of hydration and pozzolanic reaction. In addition the band at 1650 cm^{-1} is related to the bending v_2 of H_2O and indicates the formation of CSH [34]. The band at 994 cm^{-1} is due to CSH which increases from 3 days up to 90 days. Also, the band decreases with curing time up to 28 days, this due to the transformation of ettringite to monosulfate hydrate phase, which is shifted at lower frequency with curing time at 90 days to become 468 cm^{-1}. The absorption band at 1424 cm^{-1} is due to the presence of $_3\ CO_3^{2-}$ as well as 876 cm^{-1} (v_2) and 712 cm^{-1} (v_4) that form from carbonation of $Ca(OH)_2$.

Bulk density

The bulk density of cement pastes cured up to 90 days is plotted in Figure 21. It is clear that as the slag was replaced by GCB (10 mass (S1)) the bulk density decreases. This is due to two factors; the first is due that the slag has higher density than GCB, while the second is due to the increase of water of consistency. Mix S2 (10 mass GCB +10 mass WCS +10 mass SF) cement paste give lower bulk density. As the silica fume content increases the bulk density decreases. This is also due to the increase of the water of consistency which increases the porosity and then decreases the bulk density.

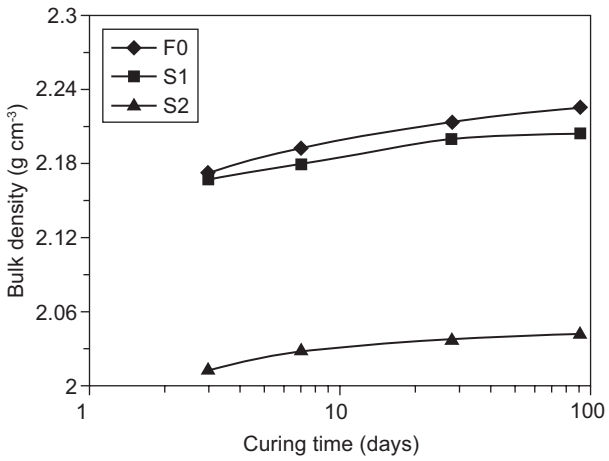

Figure 21. Bulk density of WCS–GCB–SF cement pastes with curing time.

Total porosity

Total porosity of cement pastes cured up to 90 days are graphically plotted in Figure 22. It is clear that the total porosity decreases with curing time due to the continuous hydration and filling some of available open pore volumes. Replacement of 10 mass % WCS by 10 mass % GCB the total porosity decreases. This is due to that the GCB is more pozzolanic than the slag and to the presence of quartz which acts as a nucleating agent that accelerates the rate of reaction [25-27]. GCB forms more hydration products to fill some pores between the cement particles; hence the total porosity decreases up to 90 days. As the slag was replaced by another 10 mass % SF in addition to 10 % GCB (S2), the total porosity was increased up to 90 days, due to the increase of water of consistency.

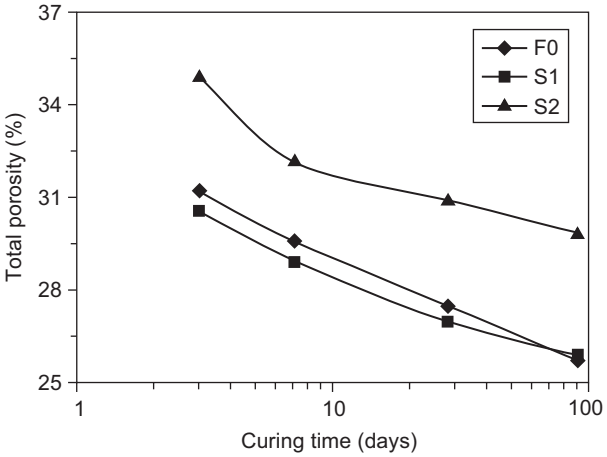

Figure 22. Total porosity of WCS–GCB–SF cement pastes up to 90 days.

Compressive strength

Compressive strength of hardened cement pastes are graphically represented in Figure 23. The compressive strength of cement pastes increases with curing age, due to the decrease of the total porosity and increase of bulk density. The compressive strength of slag cement 30 mass % (F0) is higher than other cement pastes. Replacement of WCS by 10 % GCB (S1) decreases the compressive strength after 7 days due to the increase of mixing water, whereas the replacement of WCS by 10 mass % GCB and 10 mass % SF (S2), the compressive

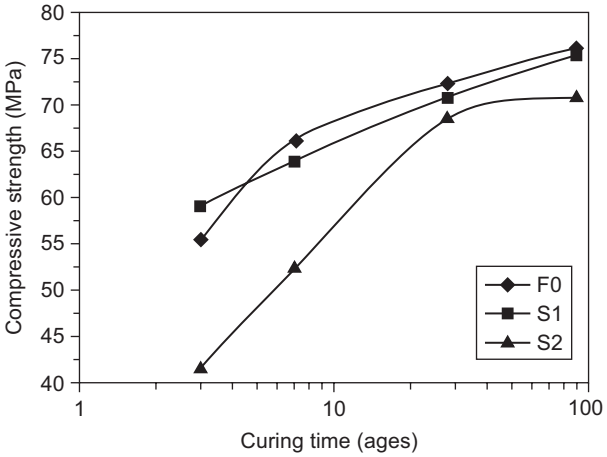

Figure 23. Compressive strength of cement pastes cured up to 90 days.

strength also decreases. This mix contain 10 mass % SF which need mixing water than the other two mixes free from SF (26.7 % for mix F0 to 31.0 % for mix S2), due to the high surface area.

The decrease of compressive strength of S2 with 10 mass % SF is due to the increase of water of consistency. On the other side, there is small difference between F0 (30 mass % WCS) and S2 (20 mass % WCS + 10 mass % GCB) only after 3 days. The decrease of compressive strength of cement pastes F0 (30 mass % WCS) is mainly due to the low pozzolanic activity of WCS in comparison with GCB. The substitution of 10 mass % WCS tends to increase the compressive strength due to the nucleating effect of GCB from the presence of quartz. Also, the decrease of cement paste with 20 mass % WCS + 10 mass % GCB mainly due to the increase of water of consistency in comparison with cement paste with only 30 mass % WCS.

CONCLUSIONS

From the above findings it can be concluded that:

1. Blended cements containing GCB and SF

Replacement of 10 mass % GCB with SF accelerates the hydration of cement paste, due to the activity of SF in comparison with GCB. The increase of SF on the expanse of GCB, the initial and final setting time is elongated and increases the chemically combined water content, due to the higher pozzolanic activity of SF in comparison with GCB. The weight losses from the decomposition of C–S–H, CAH and CASH were increased with SF content up to 10 - 20 mass %, whereas, the weight loss of portlandite and $CaCO_3$ decreases up to 30 % mass % SF.

2. Blended cements containing WCS and SF

The replacement of 10 % WCS with SF tends to accelerate the initial setting time. Increase of SF content up to 20 - 30 mass %, the initial and final setting time elongated as well as enhances the chemically combined water, due to the high surface area of SF and formation of C–S–H by the pozzolanic reaction with liberated lime, whereas, the compressive strength decreases.

3. Substitution of WCS with GCB and SF in blended cement

Water of consistency increases with the GCB and SF. S2 (10 mass % WCS + 10 mass % GCB + 10 mass % SF) has the optimum mix accelerates initial and final setting time, increases the chemically combined water contents from 3 days up to 90 days, whereas the compressive strength also decreases due to the increase of water of consistency.

REFERENCES

1. Hewlett PC.: *Lea's Chemistry of Cement and Concrete*, John Wiley & Sons Inc., New York, 2004.
2. Boldyrev VV., Pavlov SV., Goldberg EL.: Int. J Miner. Process *44–45*, 181 (1996).
3. Juhasz AZ., Opoczky L.: *Mechanical Activation of Minerals by Grinding: Pulverizing and Morphology of Particles*, Ellis Horwood, NY (1994).
4. Heikal M., El-Didamony H., Ali AH.: Indian Journal of Engineering & Material Science *7*, 154 (2000).
5. Heikal M., El-Didamony H.: Mans. Sci. Bull. Suppl. *1*, 79 (1999).
6. El-Didamony H., Heikal M., Shoaib MM.: Silicates Industrials *65*, 39 (2000).
7. Heikal M., El-Didamony H., Morsy MS.: Cement and Concrete Research *30*, 1827 (2000).
8. Heikal M.: Cement and Concrete Research *30*, 1835 (2000).
9. Heikal M., El.Didamony H., Mostafa M.: Silicates Industrials *74*, 155 (2009).
10. Heikal M.: Building Research Journal *56,* 157 (2008).
11. Langan BW., Weng K., Ward MA.: Cem. Concr. Res. *32*, 1045 (2002).
12. Kadri E., Duval R.: Constr. Build Mater. *23*, 3388 (2009).
13. Wang A., Zhang C., Sun W.: Cement Concrete Res. *34*, 2057 (2004).
14. Zelic J., Rusic D., Veza D.: Cement Concrete Res. *30*, 1655 (2000).
15. AnMing SHE., Wu YAO.: Science China, Technological Sciences *53*, 1471 (2010).
16. 16. Rahman A., Abo-El-Enein S.A., Aboul-Fetouh M., Shehata Kh.: Arabian Journal of Chemistry, In Press, Corrected Proof (2011).
17. Nataraja MC., Nalanda Y.: Waste Manag. *28*, 1168 (2008).
18. Nochaiya, Thanongsak, Wongkeo, Watcharapong, Chaipanich, Arnon.: Fuel *89*, 768 (2010).
19. Lee, Tzen-Chin, Wang, Wei-Jer, Shih, Ping-Yu, Lin, Kae-Long.: Cem. Concr. Res. *39*, 651 (2009).
20. Bágel L.: Cem. Concr. Res. 28, 1011 (1998).
21. ASTM Standards, *Standard test method for normal consistency of hydraulic cement*, American Society for Testing and Materials, C 187-83, 195 2008.
22. Tkalcec E. and Zellic J.: Zement - Kalk - Gips *40*, 574 (1987).
23. Heikal M., Morsy MS., El-Didamony H.: Mans. Sci. Bull. Suppl. *2*, 195 (2002).
24. Heikal M., El-Didamony H., Helmy I.M., Abd El-Raoof F.: Journal of Ceramics-Silikáty *48,* 49 (2004).
25. El-Didamony H., Helmy IM., Amer AA. Heikal M.: ZKG International *48*, 502 (1995).
26. Zhang MH. Gjorv OE.: Cem. Conc. Res. *25*, 1791 (1992).
27. Mostafa NY., El-Hemaly SAS., Al-Wakeel EI., El-Korashy SA., Brown P.W.: Cem. Concr. Res. *31*, 475 (2001).
28. Mak SL., Torii K.: Cem. Concr. Res. *25*, 1791 (1995).
29. Ramachandran VS., Paroli RM., Beaudoin JJ. Degado AH.: *Handbook of thermoanalysis of construction materials*, William Andrew Puplishing, Noyes 2002.
30. Radwan MM., Heikal M.: Cem. Concr. Res. *35*, 1601 (2005).
31. Feldman RF., Ramachandran VS., Sereda PJ.: J. Am. Ceram. Soc. *98*, 20 (1965).
32. Perraki TH., Kakali Gl., Kontolean F.: Microporous and Mesoporous Materials *61*, 205 (2003).